

## Electrical properties of $\text{Ni}_{0.4}\text{Mg}_{0.6}\text{Fe}_2\text{O}_4$ ferrites

K.T.Veeranjaneaya<sup>1</sup> and D. Ravinder<sup>1, 2</sup>

<sup>1</sup>Department of Physics, National college, Bagepalli, Chikkaballapura (district), Karnataka-561207, India

<sup>2</sup>Department of Physics, Osmania University, Hyderabad- 500 007, Telangana, India

### ABSTRACT

$\text{Ni}_{0.4}\text{Mg}_{0.6}\text{Fe}_2\text{O}_4$  Ceramic samples were prepared by conventional double sintering approach and sintered at 1300°C/4 h. These ferrites are further characterized using X-ray diffractometer. The diffraction study reveals that the present compound shows perfect single phase cubic spinel structure. In addition, the behavior of distinct electrical properties such as dielectric constant ( $\epsilon'$ ), dielectric loss ( $\epsilon''$ ) and ac-conductivity ( $\sigma_{ac}$ ) as a function frequency as well as temperature is analyzed using the LCR controller.

**Keywords:** Ferrites; Sintering; X-ray Diffractometer; AC-Electrical Conductivity.

### I. INTRODUCTION

Polycrystalline ferrites are of general spinel structure  $\text{AB}_2\text{O}_4$ , where 'A' corresponds to divalent Ni, Mg, Cu, Zn, Mn and Fe and 'B' corresponds to the trivalent iron ions respectively [1]. The field of ferrites is well focused due to their potential applications as storage devices, magnetic sensors, refrigeration, photo-catalysis, drug delivery systems, magnetic resonance imaging, transformers, and inductors, shielding devices, anode materials, spintronic and electronic devices. These applications are attributed to the various electrical and magnetic properties of ferrites [2-7]. Generally, solid state reaction method is employed for the synthesis of ferrites which allows to micron sized particles.

Recently several researchers investigated electrical and magnetic properties of NiMg ferrites using various techniques such as citrate-gel [2, 3], self-combustion sol-gel [4], egg-white precursor [5], chemical co-precipitation [8, 9], self-combustion sol-gel [10] and microwave sintering techniques [1]. All these techniques well focused on reporting the variation of dielectric constant, dielectric loss tangent, ac, dc-conductivity, ac, dc-activation energies, magnetic permeability, magnetic loss, saturation magnetization, coercivity, magnetic moment and cation distribution etc., with increase of magnesium content in nickel ferrite system. The above mentioned properties are dependent of grain size, cation distribution, sintering condition, sintering method, bulk density and purity of ferrites [1].

In view of this Berchmans et al. [2, 3] reported that the ferrite composition  $\text{Ni}_{0.4}\text{Mg}_{0.6}\text{Fe}_2\text{O}_4$  can be used as a green anode material as it showed a high electrical conductivity value of 0.6 S/cm. It is well known fact that the ac-conductivity ( $\sigma_{ac}$ ) is a dependent parameter of dielectric constant ( $\epsilon'$ ), dielectric loss ( $\epsilon''$ ),

frequency and temperature [11, 12]. Therefore, the authors' have concentrated to report the effect of temperature and frequency on ( $\epsilon'$ ), ( $\epsilon''$ ) and ( $\sigma_{ac}$ ) of  $\text{Ni}_{0.4}\text{Mg}_{0.6}\text{Fe}_2\text{O}_4$  composition via conventional solid state reaction method.

### II. EXPERIMENTAL PROCEDURE

$\text{Ni}_{0.4}\text{Mg}_{0.6}\text{Fe}_2\text{O}_4$  is prepared by conventional double sintering method. The raw materials NiO, MgO and  $\text{Fe}_2\text{O}_3$  are weighed and mixed according to the stoichiometric ratio. The resultant powders are grinded in agate motors for 15 h. Furthermore, the powders are pre-sintered at a temperature of 1200°C for 14 h in conventional furnace. The pre-sintered samples are crushed into fine powder. The powder is mixed with polyvinyl alcohol (PVA) as a binder and pressed into pellets (10 mm diameter) applying 3 ton pressure. These are sintered at 1300°C for 2 h in a conventional furnace. The sintered samples are characterized using X-ray Diffractometer (Bruker X-Ray Powder Diffractometer,  $\text{CuK}\alpha$ ,  $\lambda = 0.15418$  nm) for structural investigation. HIOKI 3532-50 LCR HiTESTER (Japan) is used for studying the electrical properties.

### III. RESULTS AND DISCUSSION

The variation of intensity (I) as a function of two-theta ( $2\theta$ ) angle for  $\text{Ni}_{0.4}\text{Mg}_{0.6}\text{Fe}_2\text{O}_4$  is shown in Fig.1. It is observed from figure that the sintered ferrite at 1300°C for 2 h shows the perfect single phases. The reflection planes indexed in diffraction pattern show the formation cubic spinel structure. These are in well agreement with the standard JCPDS file number: 74-1913. The (311) plane shows the maximum intensity of 8000 among all cubic phase. The average crystallite size (D) of

(311) plane is (96 nm) calculated using the Scherrer formula [13, 14]:

$$D = 0.9\lambda/\beta\cos\theta \quad (1)$$

Where  $\lambda$  is the wavelength of radiation used,  $\beta$  is the full width half maximum (FWHM) of diffraction peaks and  $\theta$  is the diffraction angle.

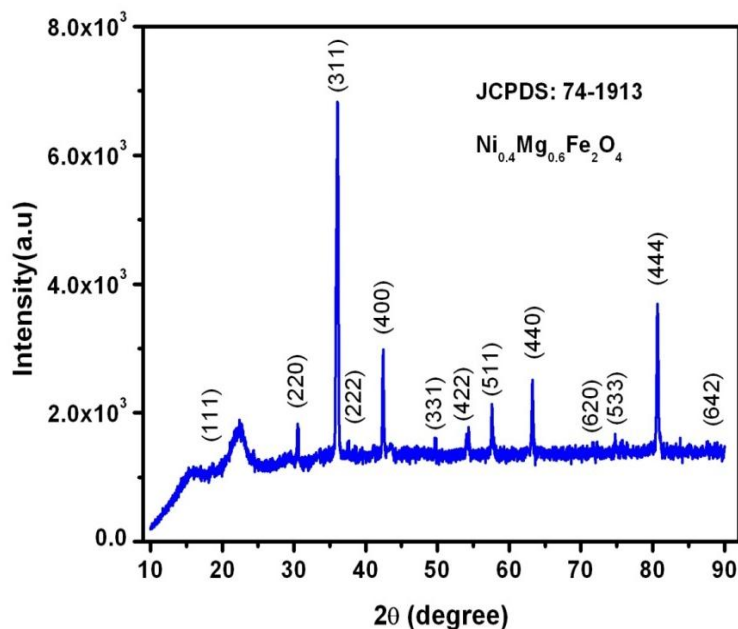


Fig.1. XRD pattern of  $Ni_{0.4}Mg_{0.6}Fe_2O_4$

The lattice constant is evaluated using a standard formula:  $a = (h^2 + k^2 + l^2)^{1/2}$ . The attributed value is of 0.8376 nm which is almost in close agreement with the reported lattice constant 0.839 nm by Naidu et al. [1]. The x-ray density  $\rho_x$  is calculated by an equation:  $\rho_x = 8M/Na^3$  where M is the molecular weight, N is the Avogadro's number ( $6.023 \times 10^{23}$  atoms/mole) and 'a' is the lattice parameter computed. The result showed that it is order  $4.925 \text{ g/cm}^3$ . The bulk density  $\rho_b$  is evaluated by using the Archimedes principle and it is found to be  $4.023 \text{ g/cm}^3$ . Furthermore, the porosity is calculated using the relation  $P = 1 - (\rho_b/\rho_x)$  and it is of 18.3 %. The low percentage of porosity expresses a fact that the ferrite sample is of high pure in nature [15].

Fig.2 shows the variation of dielectric constant as a function of temperature at different frequencies. It is seen from the figure that the ferrite composition performs a steady trend during 300 to 500 K temperatures for the selected frequencies. This can be happened due to unavailability of ferrous ions at octahedral B-sites [2]. In addition, the thermal energy among the magnetic dipoles becomes insufficient to activate the charge carriers in the applied field direction. But beyond 500 K, the plot exhibits a gradual increasing trend of dielectric constant. This kind of behavior is attributed to the faster response of charge carriers with increasing temperature i.e. the

thermal energy is allowing the dipoles to orient in the direction of the field. At very higher temperatures, the sample shows the relaxation which may be occurred due to the accumulation of charge carriers at the grain boundary interface. It is also clear that with increase of applied frequency the dielectric constant as well as relaxation is going to be suppressed. This is owing to the lagging of response of electric dipoles to the applied field. Moreover, according to Koops theory the grain boundaries are more active at lower frequencies whereas the grains are more active at higher frequencies. Therefore, the high value of dielectric constant is established at lower frequency and it is low at higher frequencies. The Maxwell-Wagner interfacial or space charge polarization is also responsible for this manner [19]. The similar behavior is observed in the literature [16-18]. The ferrite expresses a small step like increase of dielectric constant at 700 K for 50 kHz and 0.1 MHz frequencies. This is because of jumping of charge carriers at that particular temperature. The loss is also performing the similar trend as that of dielectric constant as shown in Fig. 3. The similar analysis is applicable to loss versus temperature plots at selected frequencies. In over all the ferrite composition reveal low value of dielectric constant and loss at higher frequencies. This may be useful for low noise device applications [20, 21].

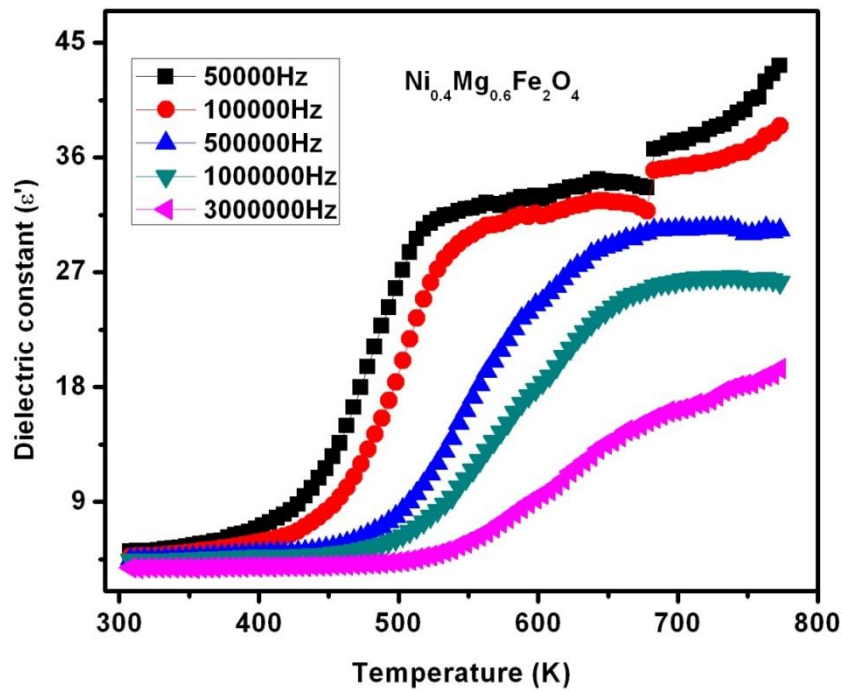


Fig.2. Temperature dependence of dielectric constant

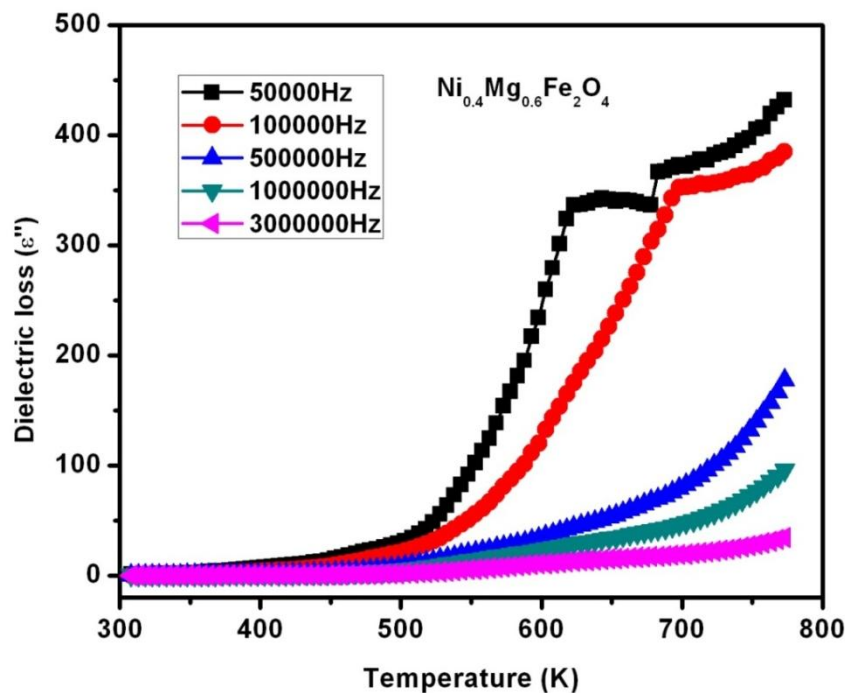


Fig.3. Temperature dependence of dielectric loss

Fig. 4 shows the temperature and frequency dependence of ac-conductivity of present ferrite composition. It is understood from the plot that the ac-conductivity is constant throughout the variation of temperature up to 500 K. At low temperatures this can be established due to the constant hopping rate of charges between ferric and ferrous ions. Above 500 K, the conductivity shows

a sharp and linear increasing trend. This indicates that the present ferrite is of magnetic semiconductor nature. The variation of ac-conductivity with respect to temperature follows the Arrhenius law:  $\sigma = \sigma_0 \exp(-E_a/K_b T)$  where  $\sigma_0$  is a pre-exponential factor,  $K_b$  is Boltzmann constant and  $T$  is absolute temperature. Therefore,  $\ln \sigma$  versus  $10^3/T$  plots as shown in Fig.6 are drawn to

find the ac-activation energies of ferrite composition at selected frequencies. In the  $\ln\sigma$  versus  $10^3/T$  plots two slopes are observed. There are different reasons behind performing two slopes or activation energies. Manjula et al. [22] reported that two slopes are because of change of conduction mechanism before and after Curie-transition temperature ( $T_c$ ). Islam et al [23] and Hiti [24] revealed that the slope of gradient line must change on passing through  $T_c$  due to change of exchange interaction between inner and outer electrons at Curie-transition temperature. The activation energies corresponding to the two slopes are evaluated using the following equation:

$$E_a = \text{slope} \times K_b \times 10^3 \text{ eV} \quad (2)$$

Where slope is  $\ln\sigma/(10^3/T)$  and  $K_b$  is Boltzmann constant ( $8.6 \times 10^{-5}$  eV). The results are listed in Table.1. It is seen that ac activation energies are decreasing with increasing of frequency which may be due to increase of ac-conductivity. The similar kinds of results are noticed in the literature [6]. The activation energies in paramagnetic region ( $E_1$ ) are higher than those in ferri magnetic region ( $E_2$ ) (Table.1). Moreover, the change of activation energies can be attributed to the change of conduction mechanism from polaron to hopping as reported by Gabal et al. [5]. The lower activation energies ( $E_2$ ) are attributed to magnetic disordering owing to limited availability of charge carriers [6].

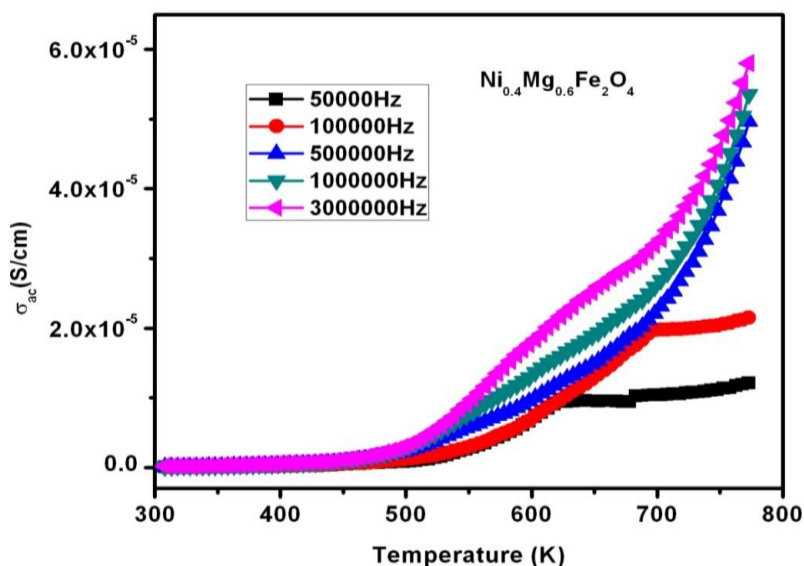
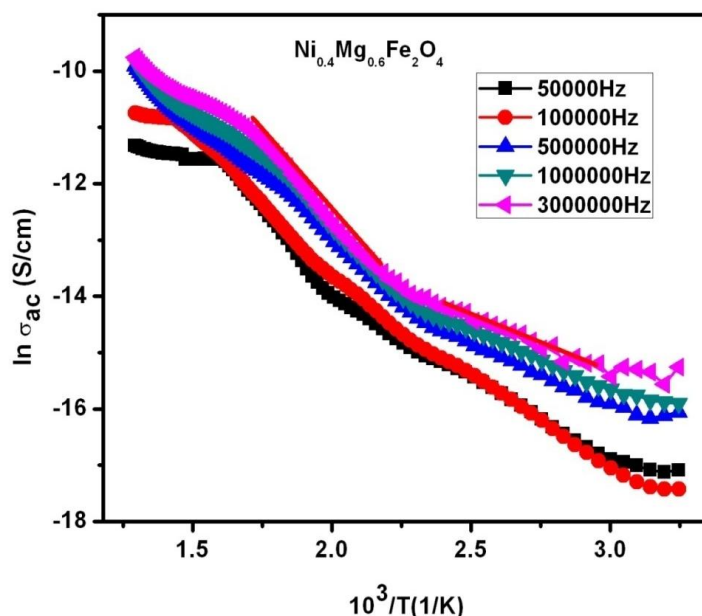


Fig.4. Temperature dependence of ac-conductivity



**Fig.5.** Arrhenius plots of  $\text{Ni}_{0.4}\text{Mg}_{0.6}\text{Fe}_2\text{O}_4$

**Table.1** The two region activation energies at selected frequencies

Frequency	$E_1$ (eV) (I)	$E_2$ (eV) (II)
50 kHz	0.439	0.271
0.1 MHz	0.410	0.259
0.5 MHz	0.382	0.211
1 MHz	0.318	0.174
3 MHz	0.293	0.146

#### IV. CONCLUSIONS

$\text{Ni}_{0.4}\text{Mg}_{0.6}\text{Fe}_2\text{O}_4$  ceramic samples are prepared by conventional double sintering technique. The average crystallite size (D) is found to be 96 nm. The low dielectric constant and low loss obtained for the present composition is useful for low noise device applications. Two different activation energies at lower and high temperature regions reveal the change of conduction mechanism from polaron to hopping conduction.

#### ACKNOWLEDGEMENT

The authors are grateful to Prof. J. Siva Kumar, Head, Department of physics, Osmania University for his encouragement.

One of the author KTV is grateful to Dr. A.H. Ramarao president of NES of Karnataka, Prof. S.N. Nagaraja, Honorary Secretary NES of Karnataka, Dr. Sadananda Maiya, Honorary Secretary, NES of Karnataka and Sri Er. Venkateshreddy, Chairman National College Bagepalli and Vice president all India Engineers association.

#### REFERENCES

- [1]. K. Chandra Babu Naidu, W. Madhuri, Microwave assisted NiMg ferrites: Structural and Magnetic Properties, *Journal of Magnetism and Magnetic Materials* 420 (2016) 109–116
- [2]. L. J. Berchmens, R. K. Selvan, P. N. S. Kumar, C. O. Augustin, Structural and electrical properties of  $\text{Ni}_{1-x}\text{Mg}_x\text{Fe}_2\text{O}_4$  synthesized by citrate gel process, *Journal of Magnetism Magnetic Materials* 279 (2004) 103-110
- [3]. L. J. Berchmens, R. K. Selvan, C. O. Augustin, Evaluation of  $\text{Mg}^{+2}$ -substituted  $\text{NiFe}_2\text{O}_4$  as a green anode material, *Materials Letters* 58 (2004) 1928-1933
- [4]. Z. V. Mocanu, M. Airimioaei, C. E. Ciomaga, L. Curecheriu, F. Tudorache, S. Tascu, A. R. Iordan, NN. M. Palamaru, L. Mitoseriu, Investigation of the functional properties of  $\text{Mg}_x\text{Ni}_{1-x}\text{Fe}_2\text{O}_4$  ceramics, *Journal of Material Science* 49 (2014) 3276-3286
- [5]. M. A. Gabal, Y. M. AlAngari, H. M. Zaki, Structural, magnetic and electrical characterization of Mg–Ni nanocrystalline ferrites prepared through egg white precursor, *Journal of Magnetism Magnetic Materials* 363 (2014) 6–15
- [6]. Chandra Babu Naidu K., Madhuri W, Microwave Assisted Solid State Reaction Method: Investigations on Electrical and Magnetic Properties of NiMgZn Ferrites, *Materials Chemistry and Physics* 181 (2016) 432-443
- [7]. K. Chandra Babu Naidu and W. Madhuri, Effect of Nonmagnetic  $\text{Zn}^{2+}$  Cations on Initial Permeability of Microwave-treated NiMg Ferrites, *International Journal of Applied Ceramic Technology*, 1–6 (2016), DOI:10.1111/ijac.12571
- [8]. H. Moradmard, S. F. Shayestech, P. Tohidi, Z. Abbas, M. Khalegi, Structural, magnetic and dielectric properties magnesium doped nickel ferrites nano particles, *Journal of Alloys and Compounds* 650 (2015) 116-122
- [9]. M. Naeem, N. A. Shah, I. H. Gul, A. Maqsood, Structural, electrical and magnetic characterization of Ni-Mg spinel ferrites, *Journal of Alloys and Compounds* 487 (2009) 739-743
- [10]. Mirela Airimioaei, Mircea Nicolae Palamaru, Alexandra Raluca Jordan, Patrick Berthet,
- [11]. Claudia Decorse, Lavinia Curecheriu and Liliana Mitoseriu, Structural Investigation and Functional Properties of  $\text{Mg}_x\text{Ni}_{1-x}\text{Fe}_2\text{O}_4$  Ferrites, *Journal of American Ceramic Society* 97 (2014) 519–526
- [12]. K. Chandra Babu Naidu, T. Sofi Sarmash, M. Maddaiah, P. Sreenivasula Reddy, D. Jhansi Rani and T. Subbarao, Synthesis and Characterization of MgO- doped  $\text{SrTiO}_3$  Ceramics, *Journal of The Australian Ceramic Society* 52 (2016) 95 – 101
- [13]. K. Chandra Babu Naidu, T. Sofi Sarmash, V. Narasimha Reddy, M. Maddaiah, P. Sreenivasula Reddy and T. Subbarao, Structural, Dielectric and Electrical Properties of  $\text{La}_2\text{O}_3$  Doped  $\text{SrTiO}_3$  Ceramics, *Journal of The Australian Ceramic Society* 51 (2015) 94 – 102
- [14]. V. Narasimha Reddy, K. Chandra Babu Naidu, T. Subba Rao, Structural, Optical and Ferroelectric Properties of  $\text{BaTiO}_3$

- Ceramics, Journal of Ovonic Research 12 (2016) 185- 191
- [15]. M. Maddaiah, A. Guru Sampath Kumar, L. Obulapathi, T. Sofi Sarmash, K. Chandra Babu Naidu, D. Jhansi Rani, T. Subba Rao, Synthesis and Characterization of Strontium Doped Zinc Manganese Titanate Ceramics, Digest Journal of Nano materials and Biostructures 10 (2015) 155-159
- [16]. M. Maddaiah, K. Chandra Babu Naidu, D. Jhansi Rani, T. Subbarao, Synthesis and Characterization of CuO-Doped SrTiO<sub>3</sub> Ceramics, Journal of Ovonic Research 11 (2015) 99-106
- [17]. M.R. Bhandare, H.V. Jamadar, A.T. Pathan, B.K. Chougule, A.M. Shaikh, Dielectric properties of Cu substituted Ni<sub>0.5-x</sub>Zn<sub>0.3</sub>Mg<sub>0.2</sub>Fe<sub>2</sub>O<sub>4</sub> ferrites, Journal of Alloys and Compounds 509 (2011) L113–L118
- [18]. K. Chandra Babu Naidu, T. Sofi Sarmash, M.Maddaiah, V.Narasimha Reddy and T.Subbarao, structural and dielectric properties of CuO-doped SrTiO<sub>3</sub>, AIP Conference Proceedings 1665 (2015) 040001; doi: 10.1063/1.4917614
- [19]. K. C. Babu Naidu, T.Sofi Sarmash, M. Maddaiah, A. Gurusampath Kumar, D. Jhansi Rani, V. Sharon Samyuktha, L. Obulapathi, T.Subbarao, Structural And Electrical Properties of PbO - Doped SrTiO<sub>3</sub> Ceramics, Journal of Ovonic Research 11 (2015) 79-84
- [20]. D Kothandan, R. Jeevan Kumar, Investigations on Electrical and Thermal Properties of Rare Earth Doped BiZnSr Borate Glasses, Journal of The Australian Ceramic Society 52 (2016) 156-166
- [21]. S. Anil Kumar, K. Chandra Babu Naidu, Structural and Dielectric Properties of Bi<sub>2</sub>O<sub>3</sub> Doped SrTiO<sub>3</sub> Ceramics, International Journal of ChemTech Research 9(1) (2016) 58-63
- [22]. S. Prathap, K. Chandra Babu Naidu, and W. Madhuri, Ferroelectric behaviour of microwave sintered iron deficient PbFe<sub>12</sub>O<sub>19-δ</sub>, AIP Conference Proceedings 1731 (2016) 030019; doi: 10.1063/1.4947624015
- [23]. R. Manjula, V.R.K. Murthy, J. Sobhanadri, Electrical conductivity and thermoelectric power measurements of some lithium–titanium ferrites, Journal of Applied Physics 59 (1986) 2929–2931
- [24]. R. Islam, M.A. Hakim, M.O. Rahman, H. Narayan Das, M.A. Mamun, Study of the structural, magnetic and electrical properties of Gd-substituted Mn–Zn mixed ferrites, Journal of Alloys and Compounds 559 (2013) 174–180
- [25]. M.El Hiti, Dielectric behavior and ac-conductivity of Zn-substituted Ni-Mg ferrites, Journal of Magnetism and Magnetic Materials 164 (1996) 187-196